Complete Induction of Autophagy is Essential for Cardioprotection in Sepsis

Chi-Hsun Hsieh, MD, Pei-Ying Pai, MD,† Hsiang-Wei Hsueh, MSc,‡ Shyng-Shiou Yuan, MD, PhD,‡ and Ya-Ching Hsieh, PhD‡*

Objective: To investigate the entire process of autophagy in the left ventricle of septic mice, and the functional significance of autophagy by using pharmacological agents.

Background: Myocardial dysfunction is a common feature in sepsis and contributes to an increased risk of developing multiple organ failure. Autophagy functions predominantly as a prosurvival pathway in the heart during cellular stress. A dynamic process of autophagy that involves the complete activation of autophagy from autophagosome formation to fusion with lysosomes has driven the development of new approaches to detecting autophagy.

Methods: Male mice were subjected to cecal ligation and puncture (CLP) or sham operation. At 1 hour after CLP operation, mice received either rapamycin (induction of autophagy), bafilomycin A1 (inhibition of autophagosomal degradation), or vehicle.

Results: The formation of autophagosomes was increased whereas the degradation of autophagosomes was decreased in the left ventricle at 24 hours after CLP. This was consistent with the morphologic finding that septic hearts revealed an increase in autophagosomes but few autolysosomes, indicating incompletion of the autophagic process. Rapamycin, which induced complete activation of autophagy, restored CLP-induced depressed cardiac performances. This cardioprotective effect was also seen in increased ATP levels, and decreased inflammatory responses. Bafiomycin A1, which resulted in incompletion of the autophagic process, did not show any above beneficial effects in CLP mice.

Conclusions: Incompletion of the autophagic process may contribute to sepsis-induced cardiac dysfunction. Treatment with rapamycin may serve a cardioprotective role in sepsis, possibly through the effect of complete induction of autophagy.

(*Ann Surg* 2011;00:1–11)

Numerous advances in the past have improved short-term survival of septic patients in intensive care units; despite these advances, sepsis leading to multiple organ failure still remains the major cause of death in severely injured patients who survive initial trauma, hemorrhage, or burn injury.[1–7] Myocardial dysfunction is a common feature in sepsis and contributes to an increased risk of developing multiple organ failure.[8,9] Studies have shown that 40% to +50% of septic patients with prolonged septic shock developing myocardial depression, as defined by reduced left ventricular (LV) ejection fraction and fraction shortening.[10,11] Apoptotic cell death is believed to be one of the major mechanisms of myocardial depression in sepsis.[12–14] Inhibition of such cell apoptosis by broad-spectrum caspase inhibitor has been shown to improve cardiac performance in endotoxemic rodent models.[12,13]

Recently, autophagy has been suggested to be an important mediator of the programmed cell death pathway in sepsis.[15,16] Autophagy is an important process in the heart and a defect in this process can be detrimental to the heart. Accumulation of autophagosomes has been noted in cardiac biopsies in patients with cardiac disorders, rodent models of these cardiac diseases, and isolated stressed cardiomyocytes.[17,18] In the ischemic myocardium, it has surprisingly received more attention as a cell protective mechanism. In fact, autophagy can be both a protective process and a precursor to cell death depending on intensity and duration of the insult. Although the relationship of autophagy to different pathophysiological conditions is now attracting attention, its role is still not clear; the crux of the problem is whether autophagy is a cell-protection or a cell-death mechanism.

Autophagy is a conserved process by which long-lived proteins and damaged organelles are delivered to the lysosome for degradation and recycling. During this process, a double-membrane vesicle called an autophagosome develops around a portion of the cytoplasm and organelles, such as mitochondria. The outer membrane of the autophagosome then fuses with the lysosomal membrane to form an autolysosome. Within the lysosome, the inner autophagosomal membrane and autophagosomal compartment are degraded and the resulting molecules are recycled.[16,19] The accumulation of autophagososomes can be due to a block of autophagosome-lysosome fusion rather than an upregulation of autophagy.[20] Thus, the abundance of autophagosomes may lead to incorrect conclusions, as increased numbers of autophagosomes do not always correlate with increased autophagic activity. To specifically determine the role of autophagy, the dynamic process of autophagy that involves the complete flow of autophagy from autophagosome formation to fusion with lysosomes has driven the development of new or modified approaches to detecting autophagy.[21,22]

The purpose of this study was to identify the role and the regulation of the autophagic process in cardiac dysfunction during sepsis. We identified the entire process of autophagy in the left ventricle of septic mice at different time points. Moreover, septic mice were treated with rapamycin (induction of autophagy[23]) or with bafilomycin A1 (inhibition of autophagosome-lysosome fusion[24]) to evaluate their effects on the regulation of the autophagic process, myocardial function, ATP levels, and the releases of inflammatory mediators, as well as cell death in septic mice.

MATERIALS AND METHODS

Sepsis Model

Experiments were performed on male C3H/HeN mice (6–8 weeks old; Experimental Animal Center of the National Science Council, Taiwan, ROC). Sepsis was induced by cecal ligation and puncture (CLP) as described previously.[25,26] In brief, under ether anesthesia, the cecum was exposed by a 1-cm midline laparotomy and

*Department of Trauma and Emergency Surgery; †Department of Internal Medicine, Division of Cardiology, China Medical University Hospital, China Medical University, Taichung 404, Taiwan, ROC; and ‡Department of Medical Research, E-Da Hospital, I-Shou University, Kaohsiung 824, Taiwan, ROC

Supported by E-Da Hospital grant EDAHT98011 (Ya-Ching Hsieh), National Science Council grant NSC-98–2320-B-650–001-MY2 (Ya-Ching Hsieh), and NSC 97–2314-B-039 -008 -MY3 (Chi-Hsun Hsieh).

Reprints: Ya-Ching Hsieh, PhD, Department of Medical Research, E-Da Hospital/I-Shou University, 6 Yi-Da Road, Kaohsiung county 824, Taiwan, ROC. E-mail: yaching.hsieh@gmail.com.

ISSN: 0003-4932/11/0000-0001
DOI: 10.1097/SLA.0b013e318214b67e

was ligated just below ileocecal junction. Two cecal punctures were made with a 22-gauge needle and a small amount (droplet) of feces was pressed out to ensure patency of the punctures. The bowel loops were returned to their anatomical position and the abdominal wall was closed in layers using 6–0 surgical sutures (Ethicon Inc., Somerville, NJ). Postoperatively, 1 mL of 0.9% saline was administered subcutaneously. Before and after the surgery, animals had unrestricted access to food and water. Sham-operated mice were operated identically, except that the cecum was not ligated or punctured. Twenty-four hours after surgery, the animals were killed, and hearts were removed for further evaluation. In treatment groups, rapamycin (10 mg/kg BW; BioVision, Mountain View, CA) or bafilomycin A1 (1 mg/kg BW; LC Laboratories, Woburn, MA) was administered intraperitoneally at 1 hour after CLP operation. In the vehicle-treated group, mice received the same volume of vehicle (10% DMSO, 4 mL/kg BW; Sigma) intraperitoneally. The dose of rapamycin in mice was chosen based on the dose at which rapamycin induced erythropoietin production and tumor suppression.[27,28] The dose of bafilomycin A1 chosen was based on the once daily or twice weekly dose in mice to inhibit tumor growth.[29,30] The experiments were carried out according to the guidelines of the Animal Committee of the E-Da Hospital/I-Shou University and China Medical University Hospital/China Medical University, Taiwan, ROC.

Western Blot Analysis

Left ventricle tissues were homogenized in lysis buffer comprised of 10 mM Tris-HCl (pH 7.5), 150 mM NaCl, 1 mM EDTA, 1 mM EGTA, 50 mM NaF, 0.5 mM phenylmethylsulfonylfluoride, 1 mM sodium vanadate, 1% Triton X-100, 0.5% Nonidet P-40, and 1 μg/mL of aprotinin. Tissue lysates were centrifuged at 17,000*g* for 10 minutes. An aliquot of the supernatant was used to determine protein concentration (Bio-Rad DC Protein Assay, Bio-Rad Laboratories, Hercules, CA). Protein aliquots were mixed with 4x lithium dodecyl sulfate sample buffer and were electrophoresed on SDS-polyacrylamide gels and transferred electrophoretically onto nitrocellulose paper. The membranes were immunoblotted with microtubule-associated protein light chain (LC3) (Novus Biologicals, Littleton, CO), Beclin 1 (BD Biosciences, Mountain View, CA), Rab7, high mobility group box-1 (HMGB1), lysosome-associated membrane protein-1 (LAMP-1), caspase 3 cleavage (Abcam, Cambridge, MA), Bax (Santa Cruz Biotechnology, Santa Cruz, CA), and Actin (BD Biosciences) antibodies. This was followed by the addition of horseradish peroxidase-conjugated secondary antibody. After the final wash, membranes were probed using enhanced chemiluminescence (Amersham, Piscataway, NJ) and autoradiographed. Actin was used as a loading control.

Immunofluorescence Staining

Cryosections from heart tissues (5 μm thick) were fixed in 4% formaldehyde in PBS for 15 minutes at room temperature, washed 3 times in PBS, and blocked for 1 hour at room temperature in PBS containing 2% goat serum and 0.1% Triton X-100. Primary antibody LC3 (Novus) or LAMP-1 (Abcam) were incubated in PBS containing 1% goat serum and 0.1% Triton X-100 overnight at 4°C. The sections were washed 3 times for 5 minutes in PBS and then incubated with Hilyte Fluor 488-conjugated rabbit antibody (AnaSpec, Fremont, CA) or Dylight 549-conjugated mouse antibody (Jackson ImmunoResearch, West Grove, PA) for 2 hours in PBS containing 1% goat serum and 0.1% Triton X-100. The sections were washed 3 times for 5 minutes in PBS, DAPI (4,6-diamidino-2-phenylindole) nuclear stain was then applied (0.5 μg/mL in PBS; for 5 minutes at room temperature), coverslips mounted onto glass slides, and viewed under a fluorescence microscope.

Transmission Electron Microscopy

Specimens were excised and fixed with fixative buffer containing 2% paraformaldehyde and 2.5% glutaraldehyde in 0.1 M PBS and were stored at 4°C until embedding. Tissue samples were then post-fixed in 1% phosphate-buffered osmium tetroxide and embedded in Spurr's resin. Sections were cut 0.12-μm thin and stained with 0.2% lead citrate and 1% uranyl acetate. Images were examined with a JEOL TEM-2000 EX II at 80 kV.

Echocardiography

Twenty-four hours after sham or CLP procedure, mice were lightly anesthetized by intraperitoneal injection of 2 mg/kg of Zoletil 50^{R} (Virbac Lab, France). Mice were secured in a supine position on a plastic board and the precardial chest wall was shaved. Transthoracic echocardiography was performed by use of a GE Healthcare cardiac ultrasound machine (ultrasound system -Vividi, Milwaukee, WI) with a 14-MHz transducer. The heart was first imaged in the 2-dimensional mode in the parasternal long-axis and/or parasternal short-axis views. These views were used to determine the optimal position of the M-mode cursor that was perpendicular to the ventricular septum and LV posterior wall, after which M-mode images were obtained. All primary measurements were made from images captured at the time of the study by use of the analysis software pre-installed in the machine. Both LV ejection fraction (EF) and fraction shortening (FS) were used as parameters to be compared between groups.

ATP Levels Determination

ATP content was measured by the ATP Bioluminescence Assay kit (Roche Diagnostics, Indianapolis, IN) according to the manufacturer's protocol. In brief, tissues were homogenized in lysis reagent supplied in the kit and then centrifuged at 10,000*g* for 1 minute. The supernatants were then transferred and protein concentrations were measured (Bio-Rad Laboratories). The samples were kept on ice until measurements were performed. For determination of ATP, 100 μL of luciferase reagent was added to the standards or 0.1 mg of left ventricle proteins and the measurement performed with a Luminometer Lumat LB9507 (Berthold, Wildbad, Germany).

Hypoxia-Inducible Factor 1α (HIF-1α) Measurement

HIF-1α was measured according to a previous study.[31] A commercially available ELISA kit was used to measure the levels of activated HIF-1α (R&D Systems, Minneapolis, MN). In brief, nuclear extracts were prepared by solubilizing cells in lysis buffer provided by the manufacturer and the protein concentrations of each sample were determined using the Bio-Rad Dc protein assay (Bio-Rad Laboratories). A biotinylated oligonucleotide containing a consensus HIF-1α binding site was then incubated with nuclear extracts for 30 minutes. After incubation, the HIF-1α-oligonucleotide complex was added to the wells of a plate, which was coated with HIF-1α capture antibody. After incubation for 2 hours, the unbound materials were washed away. A standard streptavidin-HRP format was used for detection and the optical densities were read at 450 nm followed by 570 nm subtraction on a spectrophotometer (Bio-Tek Instruments, Winooski, VT).

Cytokine Analysis

The concentrations of MCP-1 and IL-6 in cardiac tissue homogenates were measured by commercially available cytometric bead array (CBA) inflammation kits (BD Biosciences), according to the manufacturer's instructions. Briefly, 50 μL of mixed capture beads were incubated with 50 μL samples for 1 hour at 25°C and then 50 μL of mixed PE detection reagent was added. After incubation for 1 hour at 25°C in the dark, the complexes were washed twice and

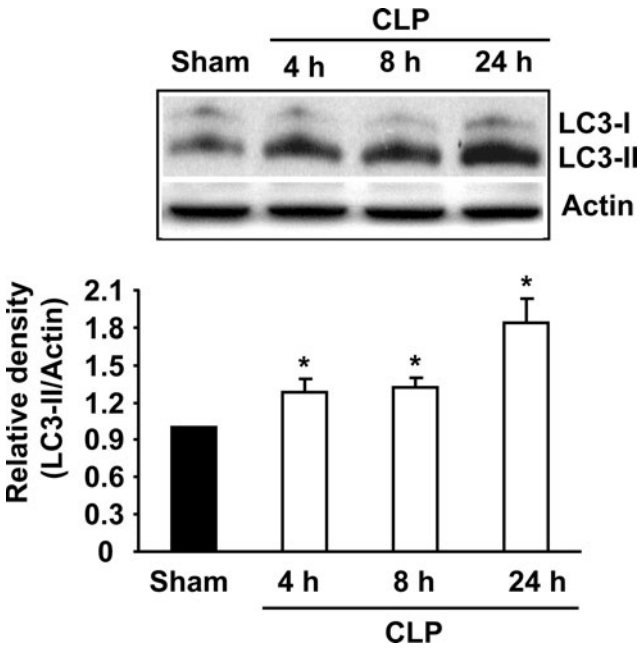

FIGURE 1. LC3-II in the left ventricle harvested 4, 8, or 24 hours after CLP. Left ventricles were harvested and tissue extracts were analyzed for LC3-II protein levels. Actin was used as a loading control. Blots obtained from several experiments were analyzed using densitometry, and the densitometric values pooled from 6 animals in each group are shown as mean ± SEM in the bar graph. Data are compared by 1-way ANOVA and Student–Newman Keul's test. LC3-II: microtubule-associated protein 1 light chain 3 (LC-3) type II; CLP: cecal ligation and puncture. $^{*}P < 0.05$ vs. Sham-operated mice.

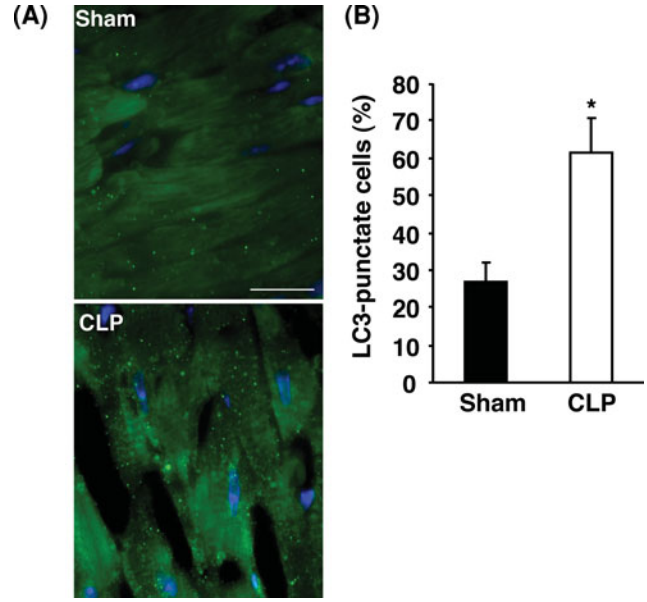

FIGURE 2. Punctate LC3 staining in the left ventricle harvested 24 hours after CLP. For the expression of punctuate LC3, heart sections were incubated with anti-rabbit LC3 antibody and then incubated with HiLyte Fluor 488-conjaugated rabbit antibody. (A) The punctate LC3 staining is characteristic of the autophagosome. CLP mice displayed numerous punctuate LC3 staining in the heart. In contrast, sham-operated heart showed only few punctate LC3 staining. Magnification: ×1000. Bar, 10 μm. (B) Quantitative evaluation of the percentage of cells expressing punctate LC3 staining. Fifteen fields were randomly selected in each sample. The number of positive cells (>10 LC3 dots per cell) was counted and the ratio of positive cells to average 100 cells was presented as percentages. Quantitative results pooled from 4 independent experiments in each group are shown as percent of total cells ± SEM in the bar graph. Data are compared by 2-tailed Student t-test. $^{*}P < 0.05$ vs. Sham-operated mice.

analyzed using the FACSCalibur flow cytometer (BD Biosciences). Data analysis was carried out using the accompanying CellQuest Pro and FCAP Array software (BD Biosciences).

Troponin I Measurement

Levels of cardiac Troponin I in the circulation were determined using a commercially available kit obtained from Life Diagnostics Inc., West Chester, PA, according to the instructions of the manufacturer.

Statistical Analysis

Data are represented as mean ± SEM. Statistical analysis of the data was performed by using 1-way ANOVA followed by Student–Newman-Keul's test. The comparison between 2 groups was analyzed by 2-tailed Student's *t*-test. $P < 0.05$ was considered to be statistically significant.

RESULTS

LC3-II at 4, 8, and 24 hours after CLP

LV tissues were harvested from mice 4, 8, and 24 hours after CLP. LC3 type II (LC3-II) was significantly increased at 4, 8, and 24 hours after CLP compared with sham-operated mice (Fig. 1). There was no significant difference in LC3-II protein levels in sham-operated mice among 4, 8, and 24 hours (data not shown).

Punctate LC3 Staining at 24 hours after CLP

LC3 was also evaluated in the left ventricle by fluorescence microscopy. In fluorescence microscopy experiments, autophagosome was evaluated by examining the punctate form (type II) of LC3. As shown in Figures 2A and B, left ventricle sections from vehicle-treated CLP mice showed an increase in punctate LC3 distribution compared with sham-operated mice.

Beclin 1, Rab7, and LAMP-1 at 4, 8, and 24 hours after CLP

LV tissues were harvested from mice 4, 8, and 24 hours after CLP. Beclin 1 was significantly increased at 8 hours whereas it was significantly decreased at 24 hours after CLP compared with sham-operated mice (Fig. 3A). Both Rab7 and LAMP-1 were significantly decreased at 4, 8, and 24 hours after CLP compared with sham-operated mice (Figs. 3B and C). There was no significant difference in Beclin 1, Rab7, and LAMP-1 protein levels in sham operated mice among 4, 8, and 24 hours (data not shown).

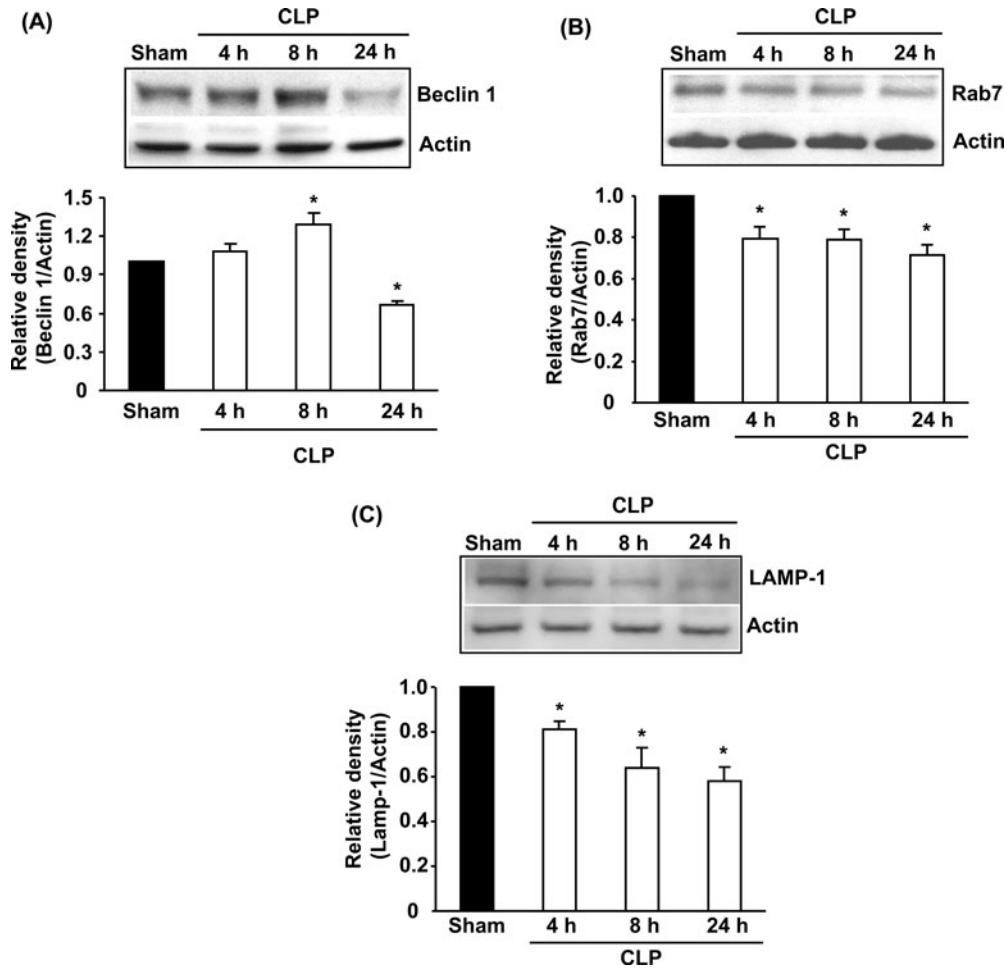

FIGURE 3. Beclin 1, Rab7, and Lamp-1 in the left ventricle harvested 24 hours after CLP. Left ventricles were harvested and tissue extracts were analyzed for Beclin 1 (A), Rab7 (B), and Lamp-1 (C) protein levels. Actin was used as a loading control. Blots obtained from several experiments were analyzed using densitometry, and the densitometric values pooled from 6–8 animals in each group are shown as mean ± SEM in the bar graph. Data are compared by 1-way ANOVA and Student–Newman Keul's test. CLP: cecal ligation and puncture. $^{*}P < 0.05$ vs. Sham-operated mice.

Autophagosome-Lysosome Fusion at 24 hours After CLP

Colocalization of lysosome (LAMP-1) and autophagosome (LC3) was observed by fluorescence microscopy. The results showed that CLP mice resulted in a reduced number of LAMP-1 staining but a markedly increased number of punctuate LC3 staining compared with sham-operated mice (Fig. 4A). Quantification of the colocalization of LC3 with LAMP-1 revealed that the ratio (LAMP-1/LC3) was significantly reduced in CLP mice compared with sham-operated mice (Fig. 4B), indicating impaired autophagosome-lysosome fusion.

Characterization of Autophagic Vacuoles at 24 hours after CLP

Autophagic vacuole was observed by transmission electron microscopy. As shown in Figure 5A, LV tissues from sham-operated mice showed normal structure with proper mitochondria distribution. In Figure 5B, CLP mice revealed cellular disorganization, myofibrillar disarray, and autophagic vacuolization. In comparison with sham animals, CLP mice exhibited an increased vacuolization. Such vacuoles were surrounded by double membranes containing cytoplasm organelles, showing common features of autophagosomes (Figs. 5B and C). An increased number of larger autophagosomes containing mitochondria (Fig. 5B) and partial digestion of autophagosomal contents with integrated double membranes (Fig. 5C) were seen in CLP mice. a representative cell in CLP mice showed an autolysosome with single-membrane containing digested cytosolic components. However, this phenomenon was only found in few cells in CLP mice (Fig. 5D). Endoplasmic reticulum-like structures which formed around portions of the cytosol and mitochondria were sporadically seen in CLP mice, suggesting the initiation of the vacuolization (Fig. 5E).

Effects of Rapamycin and Bafilomycin A1 on LC3-II, Beclin 1, Rab7, and LAMP-1

The effects of rapamaycin and bafilomycin A1 on the autophagic process in septic mice were examined. LV tissues were harvested from mice 24 hours after CLP. As shown in Figure 6A, LC3-II was significantly increased in CLP mice receiving vehicle, rapamycin, or bafilomycin A1 compared with sham-operated mice. Administration of rapamycin or bafilomycin A1 after CLP showed

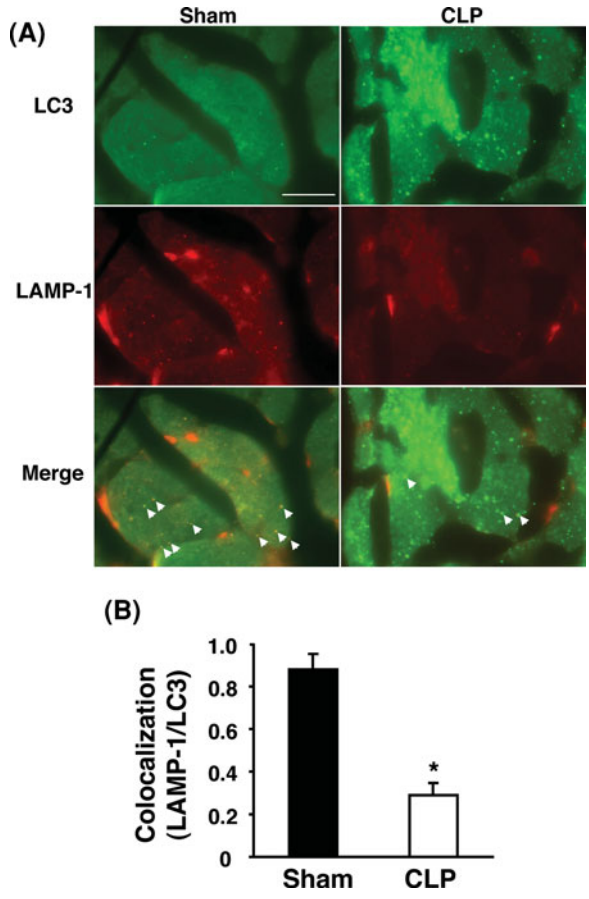

FIGURE 4. Defective autophagosome-lysosome fusion in the left ventricle harvested 24 hours after CLP. (A) Heart sections were stained with LC3 (autophagosome, green) and LAMP-1 (lysosome, red) antibodies, respectively. Colocalization of LC3 and LAMP-1 was determined. Arrows indicate colocalization of 2 stainings. Magnification: ×1000. Bar, 10 μm. (B) Quantification of the colocalization of LC3 with LAMP-1. Ten fields were randomly selected and approximately 60 cells were taken in each sample. Quantitative results pooled from 4 independent experiments in each group are shown as ratio of LAMP-1/LC3 ± SEM in the bar graph. Data are compared by 2-tailed Student's *t*-test. $^*P < 0.05$ vs. Sham-operated mice.

a further increase in LC3-II compared with vehicle-treated mice. In Figure 6B, Beclin 1 was significantly decreased in CLP mice receiving vehicle or bafilomycin A1 compared with the sham-operated group. Administration of rapamycin after CLP significantly upregulated Beclin 1 compared with vehicle-treated mice. In contrast, Rab7 and LAMP-1 were significantly decreased in CLP mice receiving vehicle or bafilomycin A1 compared with sham-operated mice (Figs. 6C and D). Administration of rapamycin after CLP significantly upregulated Rab7 and LAMP-1 compared with vehicle-treated mice (Figs. 6C and D). It should be noted that no significant difference was found in LC3-II, Beclin 1, Rab7, and LAMP-1 among sham groups with or without the treatment with rapamycin or bafiomycin A1 (data not shown).

Effects of Rapamycin and Bafilomycin A1 on Cardiac Function

LV systolic performance was assessed by LV ejection fraction and fraction shortening using echocardiography. LV ejection fraction and fraction shortening were examined at 24 hours after CLP. The result showed that CLP led to significantly depressed LV ejection fraction (Fig. 7A) and fraction shortening (Fig. 7B) compared with the sham-operated group. Administration of rapamycin after CLP restored the above parameters to levels similar to those of the sham-operated group. In contrast, bafilomycin A1 did not have such cardioprotective effects, as bafilomycin A1 treated CLP mice had similar levels of LV ejection fraction and fraction shortening compared with those of the vehicle treated CLP group (Figs. 7A and B).

Effects of Rapamycin and Bafilomycin A1 on ATP Levels

LV tissues were harvested from mice 24 hours after CLP. ATP levels were significantly decreased in CLP mice receiving vehicle or bafilomycin A1 compared with sham-operated animals (Fig. 8). Administration of rapamycin after CLP significantly increased ATP levels compared with the vehicle treated CLP group (Fig. 8).

Effects of Rapamycin and Bafilomycin A1 on HMGB1, MCP-1, IL-6, and HIF-1α

LV tissues were harvested from mice 24 hours after CLP. HMGB1 was significantly increased in CLP mice receiving vehicle or bafilomycin A1 compared with sham-operated mice (Fig. 9A). Administration of rapamycin after CLP significantly decreased HMGB1 compared with vehicle-treated mice (Fig. 9A). MCP-1 (Fig. 9B), IL-6 (Fig. 9C), and HIF-1α (Fig. 9D) levels were significantly increased in CLP mice receiving vehicle or bafilomycin A1 compared with sham-operated mice. Administration of rapamycin after CLP significantly decreased MCP-1 and IL-6 levels compared with vehicle-treated mice.

Effects of Rapamycin and Bafilomycin A1 on Apoptosis and Necrosis

Samples were harvested from mice 24 hours after CLP. LV tissues were analyzed for apoptosis proteins, Bax and caspase 3 cleavage. Plasma samples were analyzed for a myocardial specific necrotic marker, Troponin I. Bax (Fig. 10A) and caspase 3 cleavage (Fig. 10B) were significantly increased in CLP mice receiving vehicle compared with sham-operated mice. Administrations of rapamycin or bafilomycin A1 after CLP significantly decreased Bax and caspase 3 cleavage compared with vehicle-treated mice. Cardiac Troponin I (Fig. 10C) was significantly increased in CLP mice receiving vehicle or bafilomycin A1 compared with sham-operated mice. Administration of rapamycin after CLP significantly decreased Troponin I compared with vehicle-treated mice.

DISCUSSION

The role of autophagy in the heart has been controversial, and whether it is protective or harmful in the heart during sepsis is not known. As autophagy is a dynamic process, the investigation into the entire process helps us clear out the controversial role of autophagy. In this study, we investigated the autophagic process including formation and degradation of autophagosomes in the left ventricle in CLP-induced septic mice, and the functional significance of autophagy by using pharmacological agents. We found that the formation of autophagosomes was increased whereas the degradation of autophagosomes was decreased in the left ventricle at 24 hours after CLP. Observation on transmission electron microscopy also showed increased autophagosomes but few autolysosomes in

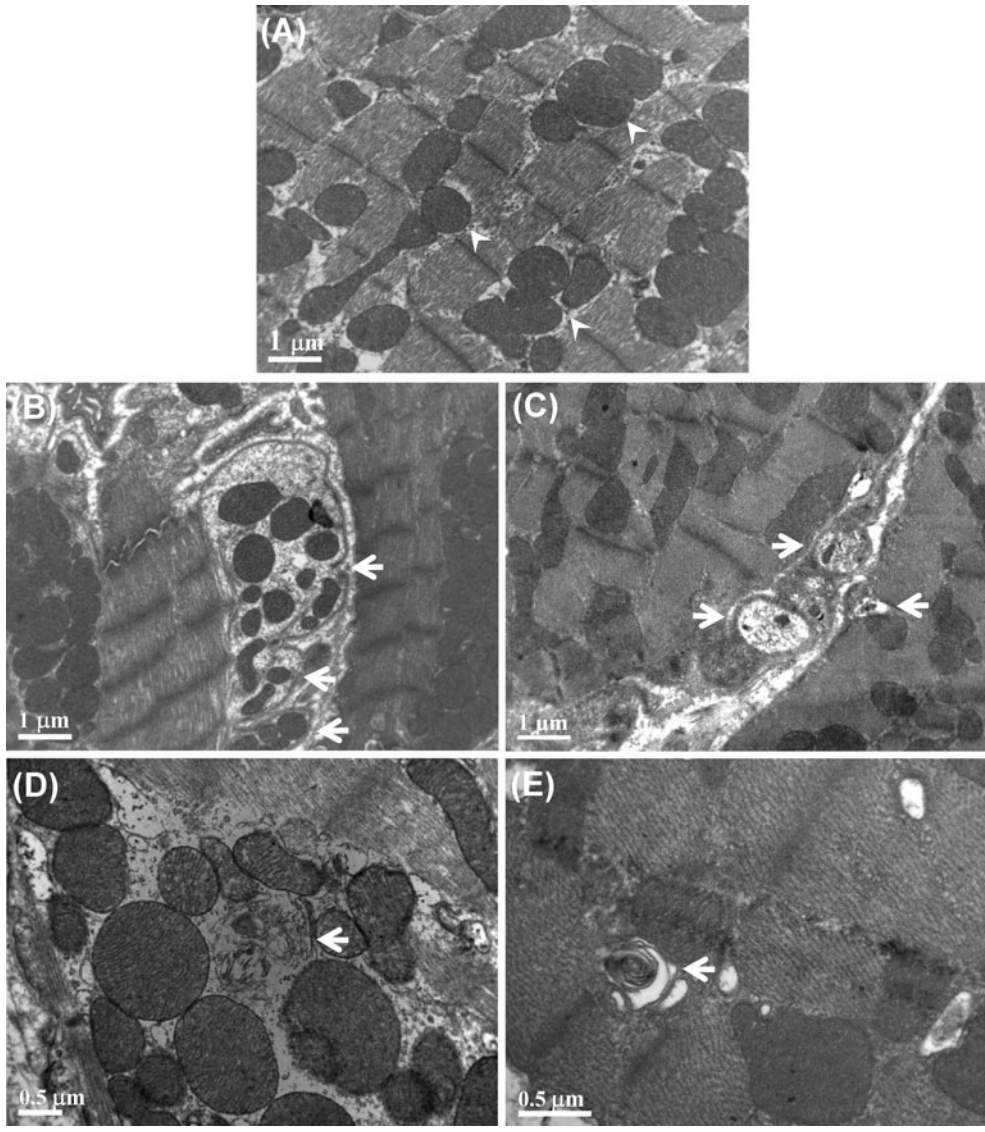

FIGURE 5. Ultrastructural features of autophagic vacuoles by transmission electron microscopy in the left ventricle harvested 24 hours after CLP. (A) cardiomyocytes are normal in appearance with proper mitochondria distribution in sham-operated mice (arrowheads); magnification: ×15,000. (B) Cellular disorganization, myofibrillar disarray, and autophagic vacuolization were seen in CLP mice. Larger autophagosomes with double-membrane structures contain engulfed mitochondria and cytoplasm materials (arrows); magnification: ×15,000. (C) Partial digestion of autophagosomal contents with integrated double membrane were seen in CLP mice (arrows); magnification: ×15,000. (D) A representative cell in CLP mice showed few cells with single-membrane autolysosomes containing digested components (arrow); magnification: ×25,000. (E) Endoplasmic reticulum-like structures surrounding mitochondria (arrow) were sporadically seen in CLP mice, suggesting the early vacuole formation; magnification: ×40,000.

CLP mice, indicating incompletion of the autophagic process. Rapamycin, which induced a complete process of autophagy, restored CLP-induced depressed LV ejection fraction and fraction shortening. Moreover, this protective effect of rapamycin was also seen in increased ATP levels, and decreased inflammatory responses, as well as decreased cardiomyocyte death in the left ventricle. Bafiomycin A1, a lysosomal inhibitor which resulted in incompletion of the autophagic process, did not show any above beneficial effects in CLP mice. These findings suggest that impairment of the autophagic process contributes to cardiac dysfunction during sepsis. Rapamycin, which results in completion of the autophagic process, may serve a cardioprotective role in sepsis.

The autophagic process requires completion of all steps of the process, to result in digestion of dysfunctional proteins or organelles. LC3 is widely used to monitor autophagosomal formation or an indication of the number of autophagosomes. There are 2 forms of LC3, including LC3-I and LC3-II. LC3-II/β-actin ratio is suggested to be more reliable than the LC3-II/LC3-I ratio, as LC3-I expression can be transcriptionally regulated and there is variability in how well LC3-I is recognized by different antibodies.[22] Beclin

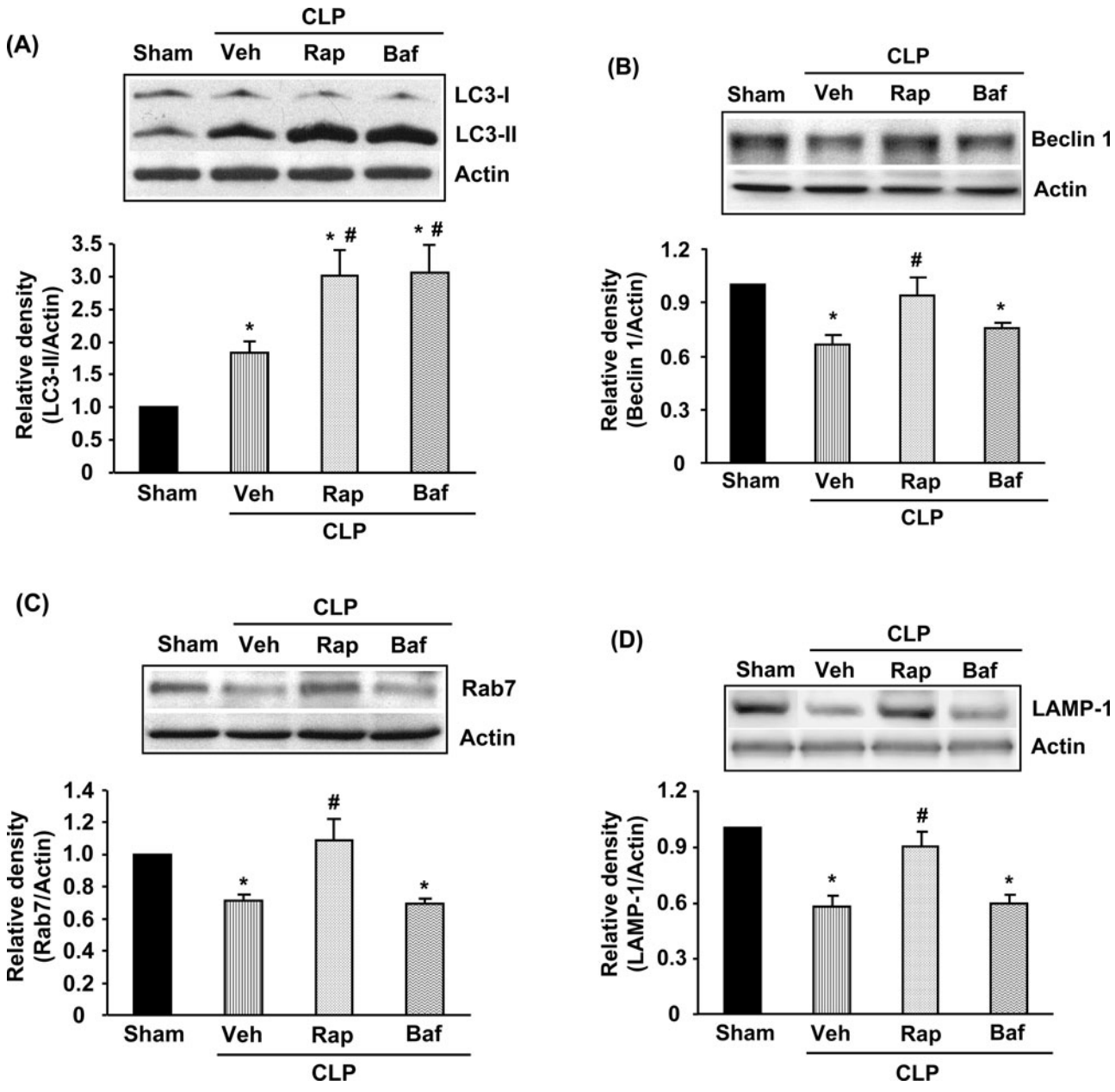

FIGURE 6. Effects of rapamycin or bafilomycin A1 on LC3-II, Beclin 1, Rab7, and Lamp-1 in the left ventricle harvested 24 hours after CLP. CLP mice were treated with vehicle (Veh), rapamycin (Rap), or bafilomycin A1 (Baf). Heart tissues were harvested and tissue extracts were analyzed for (A) LC3-II, (B) Beclin 1, (C) Rab7, and (D) Lamp-1. Actin was used as a loading control. Blots obtained from several experiments were analyzed using densitometry, and the densitometric values pooled from 6 to 8 animals in each group are shown as mean ± SEM in the bar graph. Data are compared by 1-way ANOVA and Student–Newman Keul's test. CLP: cecal ligation and puncture. $^{*}P < 0.05$ vs. Sham-operated mice. #$P < 0.05$ vs. Veh-treated CLP mice. LC3-II: microtubule-associated protein 1 light chain 3 (LC-3) type II.

1 has a key role in the autophagosome formation but has recently been found to improve autophagosome-lysosomal fusion.[32] Rab7 is required for the maturation of late autophagosomes and the fusion of autophagosomes with lysosomes.[33] LAMP-1 is a lysosome marker and its deficiency is associated with an increased accumulation of autophagic vacuoles.[34] An important concept is that the steady-state levels of LC3-II do not always reflect an alteration in the execution of the autophagic pathway.[16,21,22,35] Indeed, earlier studies which upregulation of autophgy was reported according to the increased LC3-II levels but without showing the clearance of autophagosomes need to reevaluate. Therefore, the entire process of autophagy should be taken into consideration.

In this study, septic mice exhibited increased LC3-II levels and cell numbers of punctuate LC3 staining. However, it is not clear

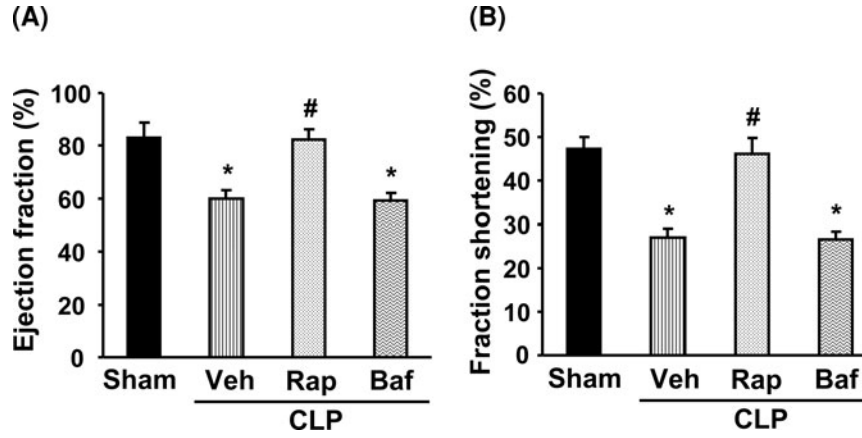

FIGURE 7. Effects of rapamycin and bafilomycin A1 on cardiac function 24 hours after CLP. Septic mice were treated with vehicle (Veh), rapamycin (Rap), or bafilomycin A1 (Baf). Cardiac function was examined by echocardiography. Left ventricle ejection fraction and fraction shortening were measured. Data pooled from 4 animals in each group are shown as mean ± SEM in the bar graph. $^{*}P < 0.05$ vs. Sham-operated mice. $\#P < 0.05$ vs. Veh-treated CLP mice.

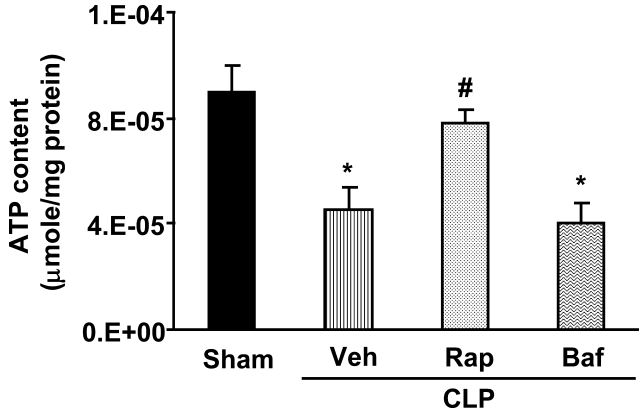

FIGURE 8. Effects of rapamycin and bafilomycin A1 on ATP levels in the left ventricle harvested 24 hours after CLP. Septic mice were treated with vehicle (Veh), rapamycin (Rap), or bafilomycin A1 (Baf). Heart tissues were analyzed for ATP contents. Values are means ± SEM of 6 animals in each group. Data are compared by 1-way ANOVA and Student–Newman Keul's test. $^{*}P < 0.05$ vs. Sham-operated mice. $\#P < 0.05$ vs. Veh-treated CLP mice.

whether this finding represents increased autophagosome formation or decreased clearance. We further found that Beclin 1, Rab7, and LAMP-1 were decreased in CLP mice except that Beclin 1 was increased at 8 hours after CLP. Moreover, impaired autophagosome-lysosome fusion was seen in CLP mice as evidenced by decreased colocalization of LAMP-1 and LC3. This was further confirmed by the finding on electron microscopy in which CLP mice revealed increased numbers of autophagic vacuoles, correlating with an increased frequency of larger autophagosomes containing mitochondria, whereas it showed few autolysosomes. These results indicate that clearance of autophagosomes is impaired in the septic heart, resulting in autophagosomal accumulation. Studies have indicated that loss of autophagy in the heart triggers LV hypertrophy, cardiac dysfunction, and eventually heart failure.[36] Accumulation of autophagosomes has also been found in cardiac biopsies in patients with cardiac disorders and experimental cardiomyocytes subjected to ischemia/reperfusion.[17,18,37] Moreover, a new concept has recently been raised that when autophagosomes or engulf targets cannot fuse with lysosomes and clear their contents, the cell may respond by ejecting the autophagosomes from the cell, thereby eliciting an acute and significant inflammatory response.[10] Thus, the consequence of accumulated autophagosomes or impaired autophagosome-lysosome fusion may contribute to sepsis induced myocardial inflammation and dysfunction.

Rapamycin is best-known to stimulate autophagy. It has been widely used to experimentally induce autophagy through its ability to block the inhibitory action of mTOR on Atg1 (autophagy-related gene 1) and autophagy.[23] An in vitro study showed that activation of autophagy by rapamycin suppressed LPS-mediated reactive oxygen species production and protected cells against LPS toxicity in HL-1 cardiomyocytes.[38] In clinical settings rapamycin has shown promise as a potential agent to inhibit restenosis after stenting of de novo coronary lesions and slow down the progression of coronary artery disease in heart transplant recipients.[39,40] In septic rats, rapamycin pretreatment decreased activation of JAK2/STAT3, HMGB1 protein, myeloperoxidase activity, and alanine aminotransferase levels, as well as improved survival.[41] Additionally, rapamycin has also been reported to reduce infarct size in a Langendorff isolated perfused rat heart model.[42] However, the protective mechanism of rapamycin and its roles in the regulation of the autophagic process in sepsis are still unknown. To test the hypothesis that autophagy might serve as a protective mechanism in the septic heart, in which the complete activation of autophagy was essential, we induced autophagy with rapamycin in CLP mice. We found that CLP mice treated with rapamycin induced completion of the process of autophagy. Moreover, treatment with rapamycin restored LV ejection fraction and fraction shortening in CLP mice. This cardioprotective effect was also found in increased ATP levels, as well as decreased HMGB1, MCP-1, IL-6, and HIF-1α levels in CLP mice. Furthermore, we tested lysosomal inhibitor bafilomycin A1 (inhibiting fusion of autophagosomes with lysosomes) in septic mice. We found that treatment with bafilomycin A1 after CLP, which showed impairment of the autophagic process, did not have any of the above cardioprotective effects. Moreover, we also measured cell apoptosis and necrosis. The results indicated that treatment with rapamycin protected against CLP-induced cardiomyocyte apoptosis and necrosis. Treatment of CLP mice with bafilomycin A1 increased necrosis but not apoptosis. These findings further support that autophagy is a protective response to sepsis-induced cardiac dysfunction and that the clearance of autophagosomes is an important step of autophagy in the septic heart. Administration of rapamycin may serve a protective mechanism in cardiomyocyte apoptosis and necrosis during sepsis, possibly through the effect of complete induction of autophagy. The reduced levels of cardiomyocyte apoptosis seen in bafilomycin A1 in comparison to vehicle treatment may be attributable to cell death necrosis occurring before apoptosis.

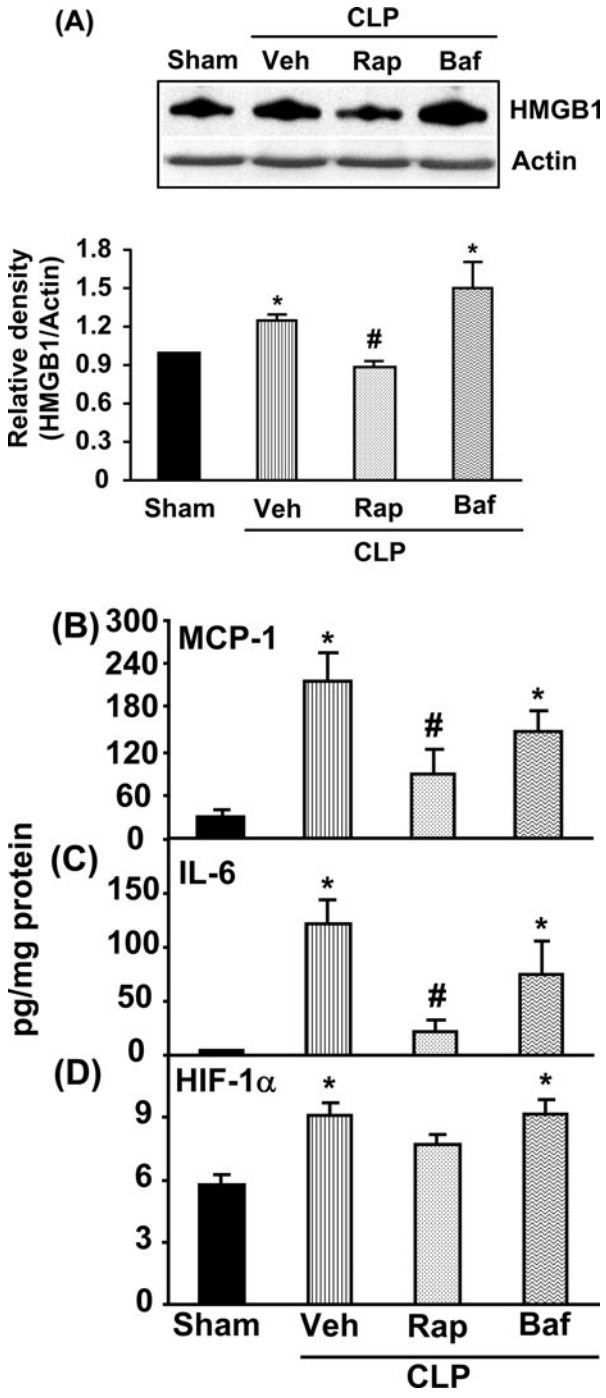

FIGURE 9. Effects of rapamycin or bafilomycin A1 on HMGB1, MCP-1, IL-6, and HIF-1α in the left ventricle harvested 24 hours after CLP. Septic mice were treated with vehicle (Veh), rapamycin (Rap), or bafilomycin A1 (Baf). Heart tissues were harvested and tissue extracts were analyzed for (A) HMGB1, (B) MCP-1, (C) IL-6, and (D) HIF-1α. Data are shown as mean $\pm$ SEM of 6 to 8 animals in each group and compared by 1-way ANOVA and Student–Newman Keul's test. $^*P < 0.05$ vs. Sham-operated mice. $\#P < 0.05$ vs. Veh-treated CLP mice.

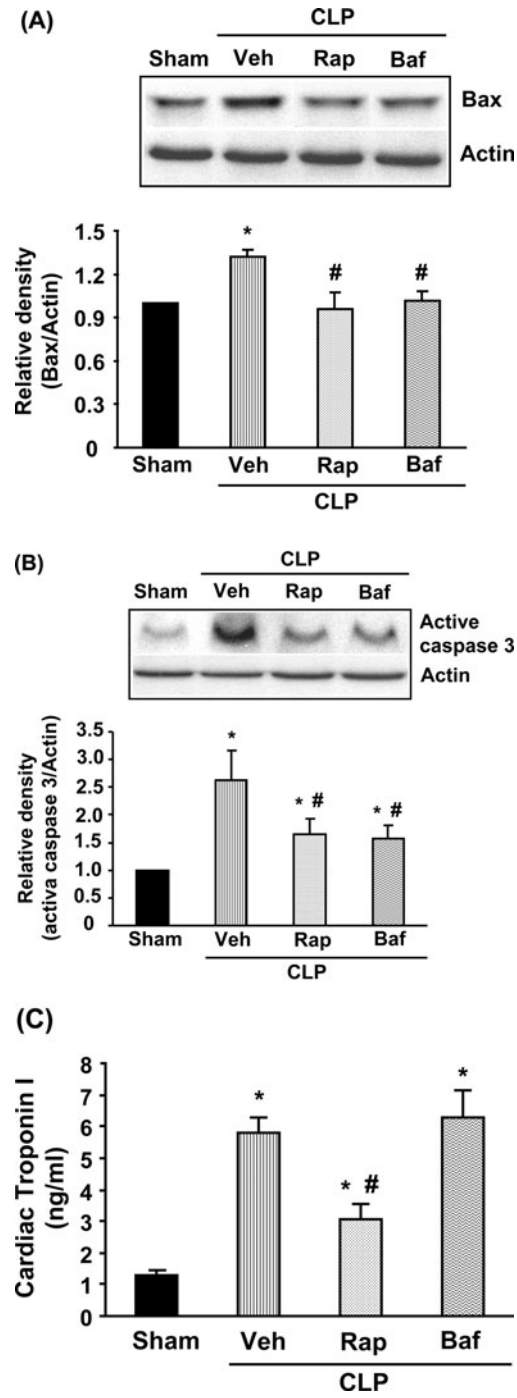

FIGURE 10. Effects of rapamycin or bafilomycin A1 on apoptosis and necrosis in the left ventricle harvested 24 hours after CLP. Septic mice were treated with vehicle (Veh), rapamycin (Rap), or bafilomycin A1 (Baf). Heart tissue extracts were analyzed for apoptotic proteins, (A) Bax and (B) caspase 3 cleavage. Plasma samples were analyzed for a necrotic marker, (C) cardiac Troponin I. Data are shown as mean $\pm$ SEM of 6 to 7 animals in each group and compared by 1-way ANOVA and Student–Newman Keul's test. $^*P < 0.05$ vs. Sham-operated mice. $\#P < 0.05$ vs. Veh-treated CLP mice.

The relationship between autophagy and cytokines is bidirectional. Interferon (IFN)-γ and TNF-α have been shown to positively regulate autophagy in macrophages and cancer cells.[43,44] In contrast, autophagy Atg16L-deficiency causes the releases of proinflammatory cytokine IL-1 from macrophages in response to endotoxin, suggesting that the increased cytokine production may reflect failure of an autophagic stress response.[45] Moreover, inhibition of mTOR by rapamycin can regulate pro- and antiinflammatory cytokine releases in immune cells, possibly via induction of autophagy.[46] In our unpublished data, we have found that upregulation of autophagy by rapamycin was accompanied by inhibiting plasma MCP-1, IL-10, and TNF-α in CLP mice. However, these effects were abolished when wortmannin (an autophagy inhibitor) was administered along with rapamycin. Thus, the effects of rapamycin on autophagy may have a role in regulating the inflammatory response in the septic heart. Nonetheless, further studies are required to fully elucidate the exact role of autophagy in the septic heart.

In summary, these findings suggest that incomplete activation of autophagy may contribute to cardiac dysfunction during sepsis. Treatment with rapamycin may serve a cardioprotective role in sepsis, possibly through the effect of complete induction of autophagy. Rapamycin may thus provide a potentially effective therapy for the prevention or treatment of sepsis related cardiac dysfunction.

REFERENCES

1. Klune JR, Billiar TR, Tsung A. HMGB1 preconditioning: therapeutic application for a danger signal? *J Leukoc Biol*. 2008;83:558–563.
2. Perl M, Chung CS, Perl U, et al. Therapeutic accessibility of caspase-mediated cell death as a key pathomechanism in indirect acute lung injury. *Crit Care Med*. 2010;38:1179–1186.
3. Macias CA, Chiao JW, Xiao J, et al. Treatment with a novel hemigramicidin-TEMPO conjugate prolongs survival in a rat model of lethal hemorrhagic shock. *Ann Surg*. 2007;245:305–314.
4. Senthil M, Watkins A, Barlos D, et al. Intravenous injection of trauma-hemorrhagic shock mesenteric lymph causes lung injury that is dependent upon activation of the inducible nitric oxide synthase pathway. *Ann Surg*. 2007;246:822–830.
5. Coimbra R, Melbostad H, Loomis W, et al. LPS-induced acute lung injury is attenuated by phosphodiesterase inhibition: effects on proinflammatory mediators, metalloproteinases, NF-kappaB, and ICAM-1 expression. *J Trauma*. 2006;60:115–125.
6. Wu R, Zhou M, Dong W, et al. Ghrelin hyporesponsiveness contributes to age-related hyperinflammation in septic shock. *Ann Surg*. 2009;250:126–133.
7. Hsieh YC, Choudhry MA, Yu HP, et al. Inhibition of cardiac PGC-1alpha expression abolishes ERbeta agonist-mediated cardioprotection following trauma-hemorrhage. *Faseb J*. 2006;20:1109–1117.
8. Kumar A, Haery C, Parrillo JE. Myocardial dysfunction in septic shock. *Crit Care Clin*. 2000;16:251–287.
9. Rudiger A, Singer M. Mechanisms of sepsis-induced cardiac dysfunction. *Crit Care Med*. 2007; 35:1599–1608.
10. Gottlieb RA, Mentzer RM. Autophagy during cardiac stress: joys and frustrations of autophagy. *Annu Rev Physiol*. 2010;72:45–59.
11. You W, Min X, Zhang X, et al. Cardiac-specific expression of heat shock protein 27 attenuated endotoxin-induced cardiac dysfunction and mortality in mice through a PI3K/Akt-dependent mechanism. *Shock*. 2009;32:108–117.
12. Carlson DL, Willis MS, White DJ, et al. Tumor necrosis factor-alpha-induced caspase activation mediates endotoxin-related cardiac dysfunction. *Crit Care Med*. 2005;33:1021–1028.
13. Neviere R, Fauvel H, Chopin C, et al. Caspase inhibition prevents cardiac dysfunction and heart apoptosis in a rat model of sepsis. *Am J Respir Crit Care Med*. 2001;163:218–225.
14. Niu J, Azfer A, Kolattukudy PE. Protection against lipopolysaccharide-induced myocardial dysfunction in mice by cardiac-specific expression of soluble Fas. *J Mol Cell Cardiol*. 2008;44:160–169.
15. Watanabe E, Muenzer JT, Hawkins WG, et al. Sepsis induces extensive autophagic vacuolization in hepatocytes: a clinical and laboratory-based study. *Lab Invest*. 2009;89:549–561.
16. Hsieh YC, Athar M, Chaudry IH. When apoptosis meets autophagy: deciding cell fate after trauma and sepsis. *Trends Mol Med*. 2009;15: 129–138.
17. Terman A, Brunk UT. Autophagy in cardiac myocyte homeostasis, aging, and pathology. *Cardiovasc Res*. 2005;68:355–365.
18. Martinet W, Knaapen MW, Kockx MM, Meyer GR. Autophagy in cardiovascular disease. *Trends Mol Med*. 2007;13:482–491.
19. Levine B, Kroemer G. Autophagy in the pathogenesis of disease. *Cell*. 2008;132:27–42.
20. Webb JL, Ravikumar B, Rubinsztein DC. Microtubule disruption inhibits autophagosome-lysosome fusion: implications for studying the roles of aggresomes in polyglutamine diseases. *Int J Biochem Cell Biol*. 2004;36: 2541–2550.
21. Barth S, Glick D, Macleod KF. Autophagy: assays and artifacts. *J Pathol*. 221:117–124.
22. Klionsky DJ, Abeliovich H, Agostinis P, et al. Guidelines for the use and interpretation of assays for monitoring autophagy in higher eukaryotes. *Autophagy*. 2008;4:151–175.
23. Takeuchi H, Kondo Y, Fujiwara K, et al. Synergistic augmentation of rapamycin-induced autophagy in malignant glioma cells by phosphatidylinositol 3-kinase/protein kinase B inhibitors. *Cancer Res*. 2005;65: 3336–3346.
24. Hamacher-Brady A, Brady NR, Gottlieb RA. Enhancing macroautophagy protects against ischemia/reperfusion injury in cardiac myocytes. *J Biol Chem*. 2006;281:29776–29787.
25. Baker CC, Chaudry IH, Gaines HO, Baue AE. Evaluation of factors affecting mortality rate after sepsis in a murine cecal ligation and puncture model. *Surgery*. 1983;94:331–335.
26. Hubbard WJ, Choudhry M, Schwacha MG, et al. Cecal ligation and puncture. *Shock*. 2005;24(Suppl 1):52–57.
27. Ye X, Rivera VM, Zoltick P, et al. Regulated delivery of therapeutic proteins after in vivo somatic cell gene transfer. *Science*. 1999;283:88–91.
28. Xing D, Orsulic S. A genetically defined mouse ovarian carcinoma model for the molecular characterization of pathway-targeted therapy and tumor resistance. *Proc Natl Acad Sci U S A*. 2005;102:6936–6941.
29. McSheehy PM, Troy H, Kelland LR, et al. Increased tumour extracellular pH induced by Bafilomycin A1 inhibits tumour growth and mitosis in vivo and alters 5-fluorouracil pharmacokinetics. *Eur J Cancer*. 2003;39: 532–540.
30. Lim JH, Park JW, Kim MS, et al. Bafilomycin induces the p21-mediated growth inhibition of cancer cells under hypoxic conditions by expressing hypoxia-inducible factor-1alpha. *Mol Pharmacol*. 2006;70:1856–1865.
31. Hsieh CH, Nickel EA, Hsu JT, et al. Trauma-hemorrhage and hypoxia differentially influence kupffer cell phagocytic capacity: role of hypoxia-inducible-factor-1alpha and phosphoinositide 3-kinase/Akt activation. *Ann Surg*. 2009;250:995–1001.
32. Zhong Y, Wang QJ, Li X, et al. Distinct regulation of autophagic activity by Atg14L and Rubicon associated with Beclin 1-phosphatidylinositol-3-kinase complex. *Nat Cell Biol*. 2009;11:468–476.
33. Gutierrez MG, Munafo DB, Beron W, Colombo MI. Rab7 is required for the normal progression of the autophagic pathway in mammalian cells. *J Cell Sci*. 2004;117:2687–2697.
34. Eskelinen EL. Roles of LAMP-1 and LAMP-2 in lysosome biogenesis and autophagy. *Mol Aspects Med*. 2006;27:495–502.
35. Kroemer G, Galluzzi L, Vandenabeele P, et al. Classification of cell death: recommendations of the Nomenclature Committee on Cell Death 2009. *Cell Death Differ*. 2009;16:3–11.
36. Nakai A, Yamaguchi O, Takeda T, et al. The role of autophagy in cardiomyocytes in the basal state and in response to hemodynamic stress. *Nat Med*. 2007;13:619–624.
37. Matsui Y, Takagi H, Qu X, et al. Distinct roles of autophagy in the heart during ischemia and reperfusion: roles of AMP-activated protein kinase and Beclin 1 in mediating autophagy. *Circ Res*. 2007;100:914–922.
38. Yuan H, Perry CN, Huang C, et al. LPS-induced autophagy is mediated by oxidative signaling in cardiomyocytes and is associated with cytoprotection. *Am J Physiol Heart Circ Physiol*. 2009;296:H470–479.
39. Hausleiter J, Kastrati A, Mehilli J, et al. Randomized, double-blind, placebo-controlled trial of oral sirolimus for restenosis prevention in patients with in-stent restenosis: the Oral Sirolimus to Inhibit Recurrent In-stent Stenosis (OSIRIS) trial. *Circulation*. 2004;110:790–795.
40. Keogh A, Richardson M, Ruygrok P, et al. Sirolimus in de novo heart transplant recipients reduces acute rejection and prevents coronary artery disease at 2 years: a randomized clinical trial. *Circulation*. 2004;110: 2694–2700.

41. Hui L, Yao Y, Wang S, et al. Inhibition of Janus kinase 2 and signal transduction and activator of transcription 3 protect against cecal ligation and puncture-induced multiple organ damage and mortality. *J Trauma*. 2009;66:859–865.
42. Khan S, Salloum F, Das A, et al. Rapamycin confers preconditioning-like protection against ischemia-reperfusion injury in isolated mouse heart and cardiomyocytes. *J Mol Cell Cardiol*. 2006;41:256–264.
43. Djavaheri-Mergny M, Amelotti M, Mathieu J, et al. NF-kappaB activation represses tumor necrosis factor-alpha-induced autophagy. *J Biol Chem*. 2006;281:30373–30382.
44. Schmid D, Munz C. Innate and adaptive immunity through autophagy. *Immunity*. 2007;27:11–21.
45. Saitoh T, Fujita N, Jang MH, et al. Loss of the autophagy protein Atg16L1 enhances endotoxin-induced IL-1beta production. *Nature*. 2008;456:264–268.
46. Saemann MD, Haidinger M, Hecking M, et al. The multifunctional role of mTOR in innate immunity: implications for transplant immunity. *Am J Transplant*. 2009;9:2655–2661.
47. Brazil MI, Weiss S, Stockinger B. Excessive degradation of intracellular protein in macrophages prevents presentation in the context of major histocompatibility complex class II molecules. *Eur J Immunol*. 1997;27:1506–1514.
48. Schmid D, Pypaert M, Munz C. Antigen-loading compartments for major histocompatibility complex class II molecules continuously receive input from autophagosomes. *Immunity*. 2007;26:79–92.

